



Co-milling of glass forming ability class III drugs: Comparing the impact of low and high glass transition temperatures

Nicolas Pätzmann^{a,b}, Josef Beránek^b, Brendan T. Griffin^a, Martin Kuentz^c,
Patrick J. O'Dwyer^{a,*}

^a School of Pharmacy, University College Cork, Cork, Ireland

^b Department Preformulation and Biopharmacy, Zentiva, k.s., Prague, Czechia

^c Institute of Pharma Technology, University of Applied Sciences and Arts Northwestern Switzerland, Muttens, Switzerland

ARTICLE INFO

Keywords:

Co-milling
Ball milling
Glass transition temperature
Drug supersaturation
Melting point depression
Glass forming ability
Croscarmellose sodium

ABSTRACT

With an increasing focus on sustainable technologies in the pharmaceutical industry, milling provides a solvent-free approach to improve drug dissolution. Milling of drugs with an excipient offers additional opportunities to achieve supersaturation kinetics. Therefore, this work aims to present insights of co-milling fenofibrate and apremilast, two good glass formers with low and high glass transition temperatures (T_g s) respectively. Drugs were co-milled with croscarmellose sodium for various process durations followed by thermal analysis, investigation of crystallinity, surface area and dissolution. The dissolution enhancement of the low- T_g glass former fenofibrate highly correlated with the process-induced increase in surface area of co-milled systems ($R^2 = 0.96$). In contrast, the high- T_g glass former apremilast lost its crystalline order gradually after ≥ 10 min of co-milling, and favourable supersaturation kinetics during biorelevant dissolution testing were observed. Interestingly, the melting point of co-milled apremilast decreased and linearly correlated with the highest measured drug concentration (C_{max}) during *in vitro* dissolution (onset temperature $R^2 = 0.98$; peak temperature $R^2 = 0.96$). The melting point depression remained stable after 90 days for apremilast, whereas fenofibrate co-milled for 20 min or more showed an increase in melting point upon storage. This study demonstrated that co-milling with croscarmellose sodium is ideally suited to good glass formers with a high T_g . The melting point depression is thereby proposed as an easily accessible critical quality attribute to estimate likely dissolution performance of drugs in dry co-milled formulations.

1. Introduction

Milling is a well-established particle size reduction technology for tackling dissolution rate-limited absorption (Brokešová et al., 2022). While milling reduces particle size to a certain extent, it can also induce disorder in the crystal lattices of processed substances (Oliveira et al., 2018; Zimper et al., 2010b). Highly disordered, amorphous drug material prepared by milling can be desirable, because it typically results in a higher apparent solubility compared to ordered crystalline forms (Descamps and Willart, 2016; Murdande et al., 2010; Stukelj et al., 2019). However, the high-energy state of the crystal lattice disorder and amorphous material can lead to stability issues (Priemel et al., 2016). Hence, stabilizing lattice disorder remains a key challenge for the pharmaceutical industry to fully exploit the potential biopharmaceutical benefits of milling (Slámová et al., 2021).

Co-milling with excipients has been demonstrated as an effective strategy to further enhance drug dissolution (Asgreen et al., 2020a; Slámová et al., 2021; Vogt et al., 2008a). The mechanisms by which excipients contribute to the drug dissolution enhancement are diverse, including the inhibition of particle agglomeration, an increase in wettability, molecular interactions and the stabilization of such produced lattice disorder on drug particles due to the milling process (Asgreen et al., 2020b; Balani et al., 2010; Chipakwe et al., 2020; Löbmann et al., 2013; Patterson et al., 2007). Several studies have shown a positive effect of co-milling on the oral bioavailability of poorly water-soluble drugs (Jagadish et al., 2010; Kasten et al., 2018; Vogt et al., 2008b). Despite those advances on a lab scale in pharmaceutical research, co-milling is not yet widely used for manufacturing enabling formulations due to the risk of residual drug crystallinity (Bhujbal et al., 2021).

* Corresponding author.

E-mail address: patrick.odwyer@ucc.ie (P.J. O'Dwyer).

<https://doi.org/10.1016/j.ejps.2025.107081>

Received 6 December 2024; Received in revised form 3 March 2025; Accepted 23 March 2025

Available online 24 March 2025

0928-0987/© 2025 The Authors. Published by Elsevier B.V. This is an open access article under the CC BY license (<http://creativecommons.org/licenses/by/4.0/>).

Amorphous drug material can be obtained in different ways (Blaabjerg et al., 2017). Milling can produce highly disordered amorphous material in the solid state by gradually disrupting the crystal lattice until a lack of long-range order is achieved, which is amorphisation on the “kinetic pathway”. However, an alternative strategy to obtain amorphous drug material is quench cooling a melt or by solvent evaporation via the “thermodynamic pathway”. Previous studies investigated drugs for their ability to form a glass using the thermodynamic pathway by classifying them according to their ability to form and remain stable as an amorphous solid after quench cooling (Alhalaweh et al., 2014; Baird et al., 2010; Blaabjerg et al., 2016; Wyttenbach et al., 2016). A subsequent elaboration of both the thermodynamic and the kinetic pathway revealed a correlation between glass forming ability classes (thermodynamic pathway) of drugs and their ease to amorphise via milling (kinetic pathway) (Blaabjerg et al., 2017). However, the addition of an excipient to a drug milling process may further impact the extent of produced crystal lattice disorder on the kinetic pathway. Therefore, studying the mechanisms of co-milling induced lattice disruption could deliver useful insights to support the design of stable co-milled formulations.

Fenofibrate, a poorly water-soluble drug, has been extensively studied using various formulation strategies to improve its oral bioavailability (Ejskjær et al., 2024; Griffin et al., 2014; Lentz et al., 2021; Suys et al., 2018). The glass transition temperature (T_g) of fenofibrate is around $-20\text{ }^\circ\text{C}$, which is far below the temperature of a common milling process (Tipduangta et al., 2015). Previous research hypothesised that a drug T_g far below the process temperature negatively impacts the extent of milling-induced crystal lattice disorder (Descamps et al., 2007; Descamps and Willart, 2016). Another poorly water-soluble drug is apremilast, which has also been tested in various formulation approaches to improve its oral absorption. (Abushal et al., 2022; Yang et al., 2021; Zhang et al., 2022). In contrast to fenofibrate, the T_g of apremilast is considerably higher than common milling temperatures (Tipduangta et al., 2015; Zhang et al., 2021). Co-milling these drugs with excipients may further influence the formation of crystal lattice disorder. The widely used tablet disintegrant croscarmellose sodium has also been shown to be effective as a co-milling co-former, making it a potentially attractive option for oral solid dosage forms (Kamil and Bayoumi, 2023).

Therefore, the objective of the current study was to explore the impact of co-milling on the crystal lattice disruption of two stable glass formers with T_g s located above and below the milling temperature. The influence of co-milling on the solid state and impact on *in vitro* dissolution testing were investigated. Finally, an approach to evaluate the degree of drug crystal lattice disorder in co-milled formulations is presented.

2. Materials and methods

2.1. Materials

Apremilast and croscarmellose sodium were kindly provided by the Zentiva Group k.s. (Prague, Czech Republic). Fenofibrate as well as the dissolution medium reagents sodium chloride, sodium hydroxide and disodium hydrogen phosphate were purchased from Sigma-Aldrich (Prague, Czechia). The Simulated Intestinal Fluids powder to prepare the dissolution medium was sourced from Biorelevant.com Ltd. (London, United Kingdom).

2.2. Sample preparation by ball milling and blending

Ball milling was performed in a vibrational ball mill (MM 200, Haan, Retsch GmbH, Germany). To prepare co-milled mixtures, 250 mg (± 0.1 mg) of fenofibrate or apremilast and 500 mg (± 0.2 mg) croscarmellose sodium were placed in a 25 mL stainless steel milling jar with three stainless steel balls (9 mm diameter). The co-milling times were 1, 2, 5,

10, 20, 30 and 60 min, while fenofibrate was additionally co-milled for total durations of 0.25, 0.5, and 1.5 min. Co-milled mixtures of both drugs were stored in closed conditions protected from light at $20\text{ }^\circ\text{C}$ and a relative humidity of 40 %. To produce milled drugs, apremilast and fenofibrate were prepared without excipient under the same ball milling conditions and a milling time of 15 min. Physical mixtures were mixed in a 250 mL glass container with an orbital mixer (Turbula type T2F, Willy A Bachofen AG, Muttenz, Switzerland). The glass container was filled with 250 mg (± 0.1 mg) of drug and 500 mg (± 0.2 mg) of croscarmellose and mixed at 50 rpm for 10 min. The unmilled drug samples were used as received.

2.3. Dissolution medium preparation

Fasted State Simulated Intestinal Fluid Version 1 (FaSSIF) was prepared in line with standard operating procedures supplied by Biorelevant.com Ltd (London, UK). The pH was set to 6.50 (± 0.1) and the medium was used within 24 h.

2.4. Biorelevant dissolution testing

Dissolution testing was performed in 250 mL FaSSIF using a USP2 apparatus with a stirring speed of 50 rpm. Fibre-optic UV probes with a path length of 10 mm were employed to measure dissolved drug concentration. The UV probes were linked to the Rainbow Dynamic Dissolution Monitor (Pion Inc., Forest Row, UK) and the second derivative of the UV absorbance of fenofibrate and apremilast used to establish calibration curves with an R^2 of > 0.99 . The calibration curves were generated with concentrated stock solutions and consisted of ten different measurement points. Calibrations ranged from 0.5 to 26.5 μgml^{-1} for fenofibrate and from 5 to 100 $\mu\text{g ml}^{-1}$ in the case of apremilast. The dose added to the dissolution experiments was approximately three times the amount soluble in 250 mL of FaSSIF at $37\text{ }^\circ\text{C}$, ensuring comparable non-sink dissolution conditions for both drugs. To determine the solubility, an excess of drug was added to FaSSIF at $37\text{ }^\circ\text{C}$ and stirred with 100 rpm. The concentration of the dissolution curve plateau was used as solubility. These measured solubility values in FaSSIF, 12.2 $\mu\text{g ml}^{-1}$ for fenofibrate and 31.5 $\mu\text{g ml}^{-1}$ for apremilast, were taken as reference for dissolution experiments. To initiate dissolution, formulations equivalent to 23.63 mg of apremilast and 9.15 mg of fenofibrate were added to the vessel, corresponding to 71 mg (± 0.1) apremilast and 27.5 mg (± 0.1) fenofibrate co-milled 33.3 % (w/w) mixtures. The dissolution experiments were carried out in quadruplicate.

2.5. Particle size distribution determination

Particle size distribution was measured of unmilled and milled drug substances with laser diffraction analysis by using the Mastersizer 2000 (Malvern Instruments Co. Ltd., Solihull, UK). Fenofibrate or apremilast was added to 50 mL water and 0.05 mL of Tween 80. After 10 min (± 30 s) of mixing and stirring, the samples were immediately placed in the Hydro S instrument. A measurement began when a stable obscuration between 10 and 20 % was achieved. The refractive index was set to 1.33 for the dispersion medium (water), 1.612 for apremilast, and 1.55 for fenofibrate. One measurement took 30 s with a stirring speed of 2100 rpm, which was repeated as triplicates to determine mean values.

2.6. Specific surface area measurements

The specific surface area of binary mixtures was determined from the adsorption isotherm using the Brunauer-Emmett-Teller method. The measurements were performed with the NOVA 2000e Surface and Pore Size Analyzer (Anton Paar QuantaTec Inc., Boynton Beach, USA). Samples were degassed for 2 h at $40\text{ }^\circ\text{C}$ in a vacuum. Specific surface area measurements were made by nitrogen adsorption at 77 K in the relative pressure range $p/p_0 = 0.05\text{--}0.30$.

2.7. X-ray powder diffraction (XRPD)

Powder X-ray diffractograms were recorded using a Bruker-AXS D8 Advance powder diffractometer (Bruker, Karlsruhe, Germany). At ambient temperature, a CuK α radiation ($\lambda = 1.5418 \text{ \AA}$) operated at 40 kV and 40 mA. The applied scan rate was $0.02^\circ \text{ s}^{-1}$ at a theta-theta geometry from 4 to 40° . Finally, the generated diffractograms were modified by standard smoothing procedures and background subtraction.

2.8. Differential scanning calorimetry (DSC)

Differential scanning calorimetry was based on a Discovery DSC (Waters TA instruments, New Castle, USA). Samples were weighed in triplicates between 3 and 8 mg in a standard aluminium pan with an accuracy of 0.001 mg. Under nitrogen atmosphere ($50 \text{ ml}\cdot\text{min}^{-1}$), prepared samples were transferred into the instrument and scanned. The instrument was heated from 0° C to 200° C with a heating rate of $5^\circ \text{ C min}^{-1}$. Additionally, the glass forming ability classes of pure drug compounds were evaluated by quench cooling the melt with a cooling rate of $20^\circ \text{ C min}^{-1}$ according to Baird et al., 2010. The recrystallization behaviour was assessed by a heating rate of $10^\circ \text{ C min}^{-1}$. The T_g s of apremilast and fenofibrate were extracted by using the midpoint of the thermal event from the quench cooled melt.

3. Results

3.1. Impact of milling and co-milling on the drug crystallinity assessed by X-ray powder diffraction

The influence of the milling and co-milling process on the crystallinity of fenofibrate and apremilast was evaluated using X-ray powder diffraction. The general diffraction patterns of both drugs milled for 15 min in the absence of an excipient remained mainly unchanged (Fig. 1). Most of the Bragg peaks after milling fenofibrate reveal a lower intensity, which could be a sign of a lower crystal order of the milled drug. However, also higher Bragg peak intensities after milling of fenofibrate were observed e.g. the two peaks between 16 and 17° and the peaks at 19 as well as 26° . These higher peak intensities after milling fenofibrate indicate changes of the crystalline arrangement. This effect was not observed for the high T_g drug apremilast, which showed a general lower Bragg peak intensity after neat drug milling.

Further, the diffractogram of milled fenofibrate showed peak broadening compared to unmilled drug. The peak broadening effect of

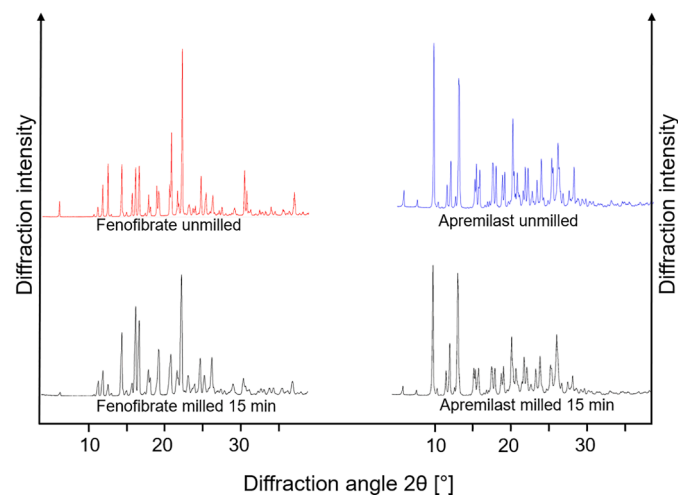


Fig. 1. X-ray powder diffractograms of fenofibrate (left, red) and apremilast (right, blue) as unmilled drug powder and both drugs after 15 min ball milling (black).

fenofibrate was more pronounced compared to the diffractograms of apremilast. Since unmilled fenofibrate particles were larger than apremilast (table S1), the higher peak broadening of milled fenofibrate may be a sign of the more greater reduction in particle size.

Co-milling fenofibrate mixtures had the same basic diffraction pattern, even after 60 min of (Fig. 2). None of the clearly visible peaks of the physically mixed mixture disappeared in diffractograms of co-milled mixtures, indicating a high degree of drug crystallinity. However, a peak broadening is also visible for co-milled fenofibrate compared to the physically blended mixture. In contrast, lower intensities of drug diffraction peaks were observed in apremilast mixtures with increased co-milling times. A reduced diffraction intensity was observed from 10 min of co-milling onwards, indicating a higher degree of drug crystal lattice disorder in co-milled mixtures. After 30 and 60 min of co-milling, almost all sharp Bragg peaks were missing in co-milled mixtures of the high- T_g glass former apremilast.

3.2. Glass forming ability class determination of fenofibrate and apremilast

The glass forming ability classification determinations of fenofibrate and apremilast are depicted in Fig. 3. During cooling of the melt, no exothermic peaks indicating recrystallization were observed for both drugs. In addition, the absence of a second crystallisation peak during reheating indicates that both compounds did not recrystallize during the entire experiment and therefore belong to glass forming ability class III. Fenofibrate had a measured T_g of -20° C (midpoint of the thermal event) at a cooling rate of $20^\circ \text{ C min}^{-1}$ whereas the determined T_g of apremilast was 76.5° C .

3.3. In vitro dissolution profiles of apremilast and fenofibrate in different formulations

Dissolution of fenofibrate as unmilled and milled drug (without excipient) displayed no significant differences in drug release after 15 and 60 min (Fig. 4), as determined by a two-sided t -test ($p > 0.05$), despite of a particle size reduction on the D10, D50 and D90 levels (table S1). The addition of croscarmellose sodium to the unmilled powder, which was physically blended for 10 min, also had no significant effect on the measured drug concentration after 15- and 60- min dissolution ($p > 0.05$). However, co-milling for 0.25 min already revealed a significant dissolution enhancement compared to the physical mixture, unmilled and milled drug, considering these two dissolution timepoints ($p < 0.05$). Prolonging the co-milling process resulted in a further significant increase in dissolution, observed up to 10 min of co-milling ($p < 0.05$). Co-milling for 10 min or longer resulted in no further significant dissolution enhancement among co-milled mixtures ($p > 0.05$).

The dissolved drug concentration of milled apremilast was significantly lower than of the unmilled drug at the 15- and 60-min dissolution timepoints ($p < 0.05$). Faster drug release was observed for the physical mixture as well as for 1- and 2- min co-milled mixtures, which showed significantly higher drug concentrations at the 15- and 60- min timepoints compared to unmilled apremilast ($p < 0.05$). Highest dissolution enhancement was measured for mixtures co-milled for 5 min and longer. After 10 min of co-milling, the dissolution profile exhibited drug supersaturation ($C_{\text{max}} = 42.05 \pm 0.31 \mu\text{g}\cdot\text{ml}^{-1}$). The maximum apparently supersaturated drug concentration grew further with the applied co-milling time up to $80.07 \pm 1.95 \mu\text{g}\cdot\text{ml}^{-1}$ for the 60 min co-milled samples, and did not fall below the equilibrium solubility (black dotted line) throughout the duration of the dissolution experiment.

3.4. Relationship between surface area of co-milled mixtures and drug dissolution

Drug dissolution of the low- T_g glass former fenofibrate, represented by the area under the dissolution curve (AUC) in the first 60 min, was in

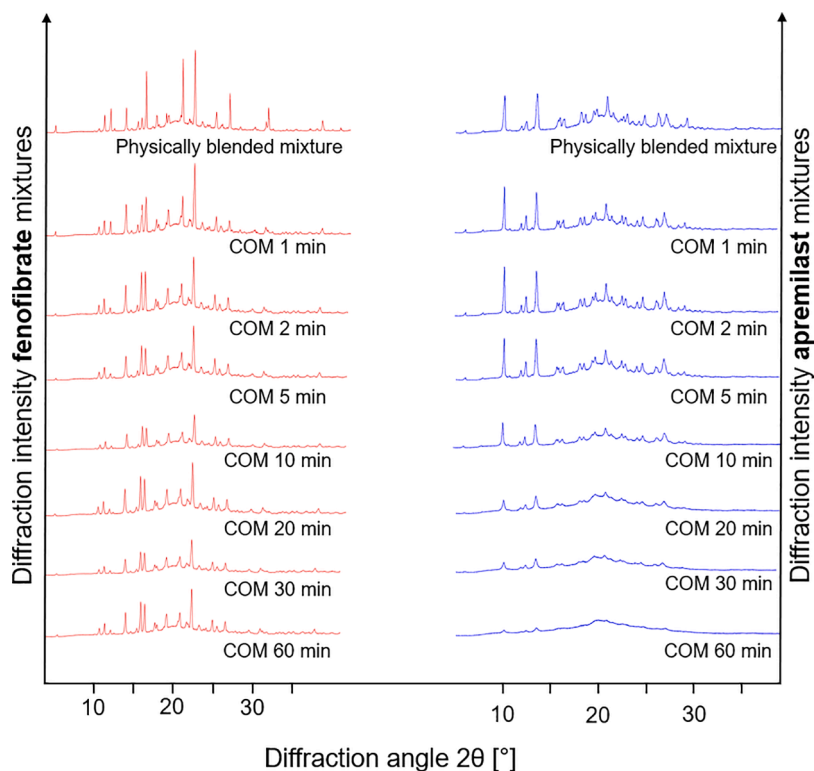


Fig. 2. X-ray powder diffractograms of fenofibrate (left, red) and apremilast (right, blue) in physically blended mixtures and co-milled mixtures (COM) at different milling times.

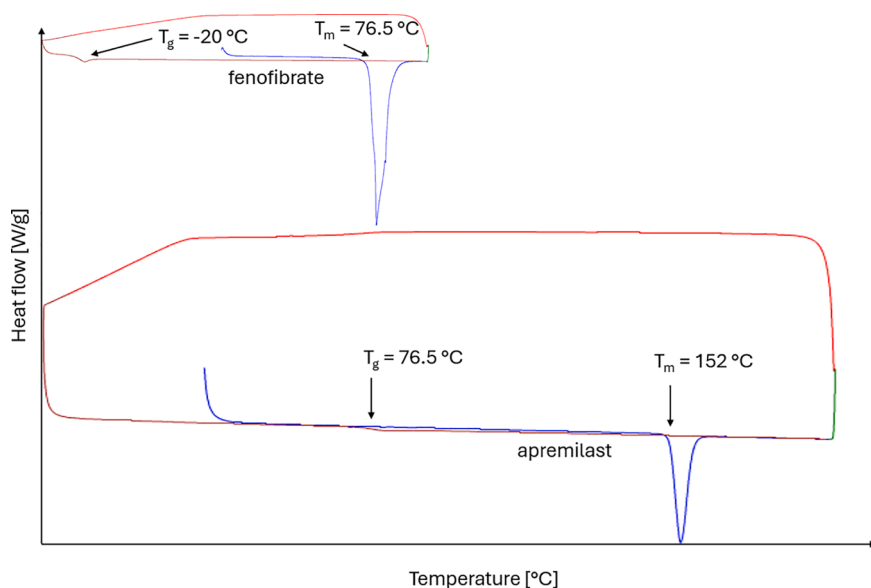


Fig. 3. Glass forming ability class determinations of apremilast and fenofibrate. The glass transition temperature (T_g) was extracted by using the midpoint of the thermal event from the quenched cooled melt and the onset of the melting peak was used to determine the melting point (T_m).

good agreement with the specific surface areas of the co-milled mixtures (Fig. 5, $R^2 = 0.96$). In contrast, the $AUC_{0-60 \text{ min}}$ of the high- T_g glass former apremilast did not correlate well with the surface area of the co-milled mixtures (Fig. 5, $R^2 = 0.07$). The relationship between co-milling time and the specific surface area is attached to the supplementary materials in figure S1.

3.5. Melting point depression of co-milled drugs and its correlation with the *in vitro* dissolution c_{max} of the high- T_g glass former apremilast

The melting point of both co-milled drugs, extracted from the onset of the melting peak from DSC thermograms, decreased to different extents (Fig. 6). While the drug melting point of the low- T_g glass former fenofibrate depressed with the processing time by around 1.5 °C after 60 min co-milling, it decreased by >10 °C for the high- T_g glass former apremilast.

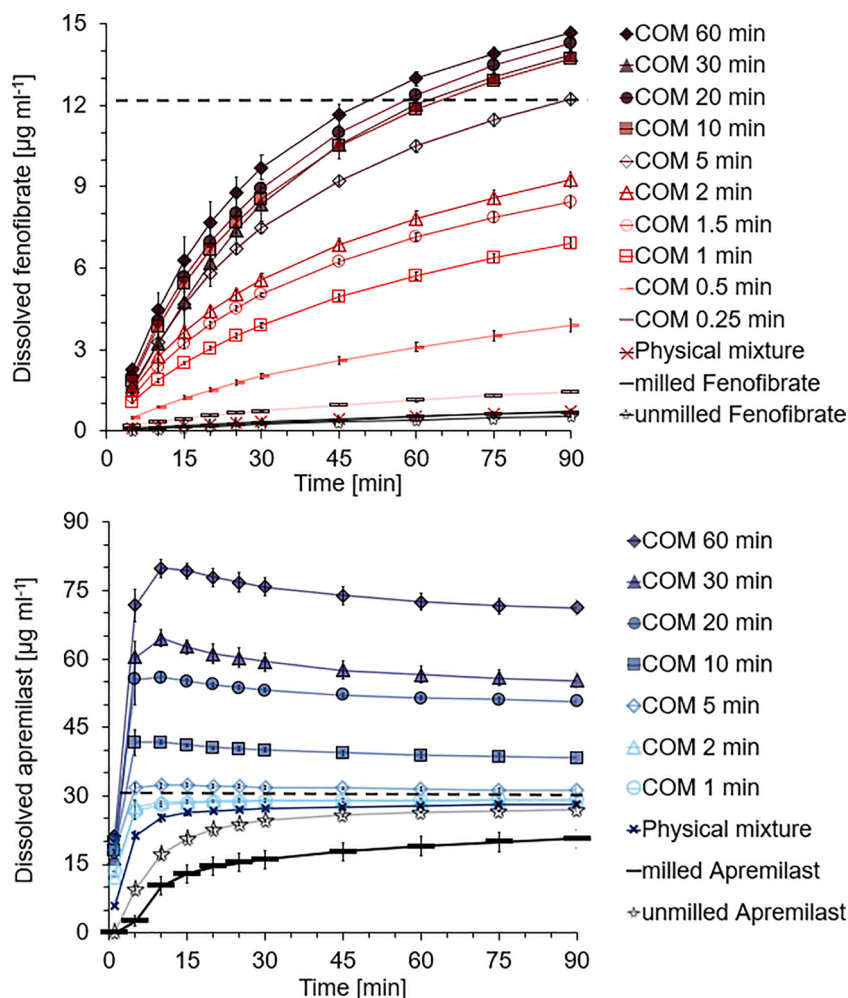


Fig. 4. Dissolution profiles of fenofibrate and apremilast as unmilled drugs, milled drugs, physically blended and co-milled mixtures (COM) at different milling times with croscarmellose sodium in a drug to excipient ratio of 1:2 (w/w). The black dotted line expresses the equilibrium solubility of the respective drugs in the used medium FaSSiF V1 at 37 °C.

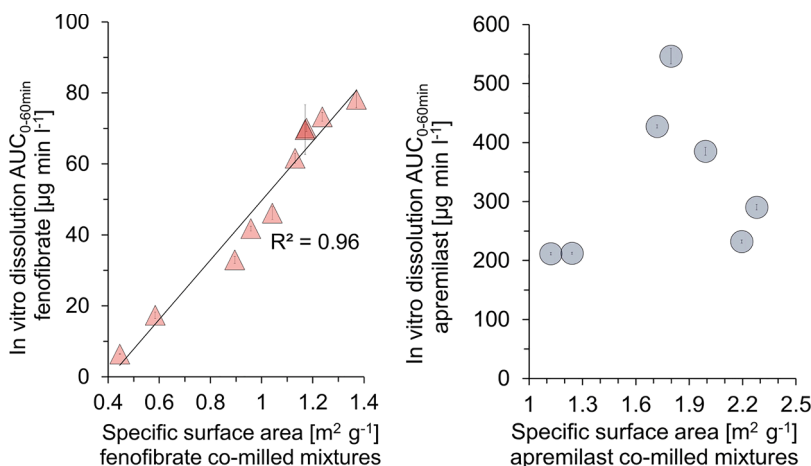


Fig. 5. Relationship of the area under the curve (AUC) of the first 60 min *in vitro* dissolution of fenofibrate (left) and apremilast (right) in co-milled mixtures at different milling times versus the specific surface area of these co-milled systems.

The dissolution profiles of Fig. 4 showed that co-milled fenofibrate dissolved according to first order kinetics whereas ≥ 10 min co-milled apremilast release profiles rather followed “spring and parachute” characteristics i.e. the drug substance supersaturated in the dissolution

medium. Subsequently, the highest measured apremilast concentration during *in vitro* dissolution (c_{max}), a parameter reflecting drug supersaturation, was chosen to relate with parameters of co-milled mixtures of apremilast. Notably, the melting point depression of co-milled

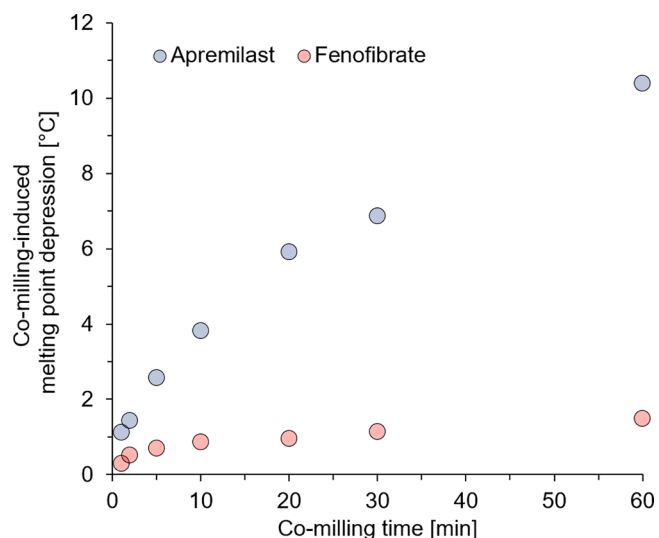


Fig. 6. Melting point depression, extracted from the onset of the drug melting peak, of co-milled apremilast and fenofibrate after various co-milling process durations.

apremilast correlated with the co-milling induced increase of the *in vitro* dissolution c_{\max} (Fig. 7). A linear relationship was observed for the onset ($R^2 = 0.98$) as well as for the tip of the melting peak ($R^2 = 0.96$).

3.6. Stability study of co-milled drugs based on the melting point depression approach

To evaluate the change in crystallinity of the drugs, stored samples were measured directly after preparation and 90 days of storage using DSC. The change in onset temperature of the melting peak of a DSC measurement was used for the evaluation (Fig. 8). No notable changes in the melting onset of co-milled fenofibrate which had been co-milled for 10 min or less were observed during storage. However, the onset of the melting peak in samples co-milled for 20 min or longer was notably higher after storage. Despite the higher co-milling induced melting point depression of apremilast, the melting point did not change noticeably for

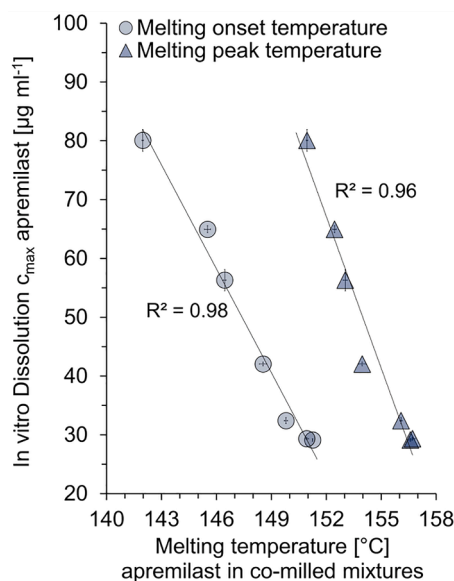


Fig. 7. The melting point depression of the high- T_g glass former apremilast as a function of the highest measured apremilast concentration (c_{\max}) during the *in vitro* dissolution process. Apremilast was co-milled with croscarmellose sodium at different milling times from one to 60 min.

all co-milled mixtures of this high- T_g glass former during storage.

4. Discussion

The aim of this study was to gain insights into co-milling of two drugs belonging to glass forming ability class III by exploring extremes in drug T_g s, which are located far below and above the milling temperature. Co-milling of the high- T_g drug apremilast led to drug supersaturation in the dissolution medium for milling times of 10 min and longer (Fig. 4), as highest measured dissolved apremilast concentration exceeded the equilibrium (crystalline) solubility of the compound in FaSSiF. In contrast, milling without an excipient did not achieve drug supersaturation and resulted in the slowest dissolution rate among all preparations (Fig. 4), which may be explained by particle aggregation (Table S1). Similar cases have also been observed in studies where compounds were milled without excipient (Pätzmann et al., 2024; Zimper et al., 2010a). The melting point of apremilast decreased with increased co-milling time, dropping by more than 10 °C after 60 min of co-milling (Fig. 6). Interestingly, the melting point depression highly correlated with the dissolution c_{\max} of apremilast during *in vitro* dissolution ($R^2 = 0.98$, melting peak onset temperature; $R^2 = 0.96$, melting peak temperature, Fig. 7). On storage, the pronounced melting point depression of this high- T_g glass former remained stable (Fig. 8). A possible explanation for the melting point depression may be the increased chemical potential of the disordered drug material, which is higher compared to the non-milled crystals, while the chemical potential of the liquid state remains the same (Ahmed et al., 2020). As a result, the energy required to melt the ball milled crystal, with a higher degree of disorder is lower and the drug material melts earlier (Alsayed et al., 2005; Chikhahia et al., 2006; Lipson and Polturak, 2024). The reduced diffraction peak intensity X-ray diffractograms of co-milled apremilast suggest the introduction of pronounced crystal lattice defects due to a processing time of ≥ 10 min (Fig. 2). Since disordered drug material appear to melt earlier, the melting point depression may be a critical quality attribute of a co-milled product to monitor the degree of crystal lattice disorder and drug supersaturation. It could therefore have applications as an easily accessible parameter in industrial settings in compliance with ICH Q8.

The melting point depression of the low- T_g glass former fenofibrate reduced by <2 °C after 60 min co-milling. This reduction is considerably less than for apremilast whose T_g is above milling temperature (Fig. 6). However, despite the lower melting point depression of co-milled fenofibrate, it did not remain stable as the melting point of samples co-milled for 20 min or more increased during storage (Fig. 8). It could be a sign of effects on the particle surfaces and may indicate reparation processes of structural disorder generated during co-milling. The dissolution rate enhancement of the low- T_g glass former fenofibrate highly correlated with the specific surface area of co-milled mixtures ($R^2 = 0.96$, Fig. 5). Sharp Bragg peaks in all diffractograms of fenofibrate containing mixtures reveal that this low- T_g glass former remained in a highly ordered crystalline state, despite 60 min of high energy dry ball milling in a stainless-steel ball mill (Fig. 2). This strengthens the hypothesis that the driving force for the dissolution enhancement of this low- T_g glass former was mainly the increase in surface area and not due to the co-milling induced drug crystal lattice disorder. Other studies showed that it was not possible to amorphise low- T_g drugs via milling (Blaabjerg et al., 2017; Descamps et al., 2007). The addition of croscarmellose sodium to the milling process appeared to not overcome this phenomenon for fenofibrate by stabilizing the crystal lattice disorder.

The dissolution enhancement of co-milled fenofibrate appears specific to the co-milling process. When fenofibrate was milled alone for 15 min, dissolution did not improve compared to the physically blended or unmilled drug, despite a reduction in particle size and an expected increase in surface area (Table S1). However, adding croscarmellose sodium during co-milling significantly improved dissolution, with effects observed after just 15 s of co-milling (Fig. 4). The superdisintegrant may

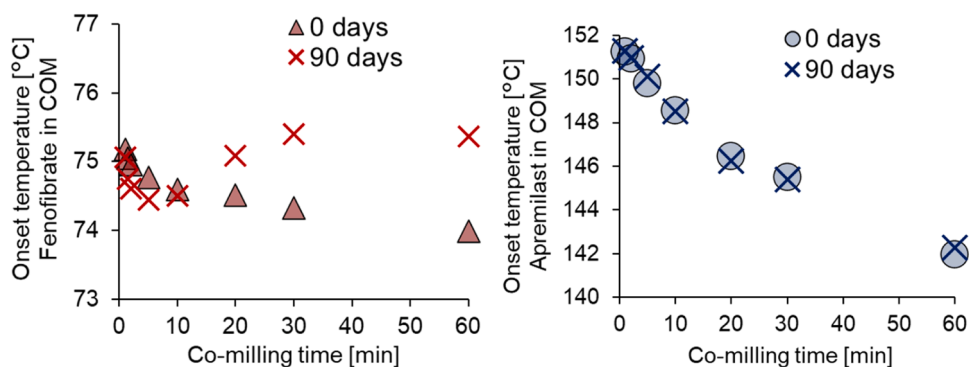


Fig. 8. Stability study of co-milled drugs using the melting point depression approach. Depicted are onset temperatures of co-milled drugs directly after preparation and after 90 days of storage under closed conditions, 20 °C and 40 % relative humidity.

have enhanced the wettability of lipophilic fenofibrate (Bennett-Lenane et al., 2021). As a result, the wettability issues of this lipophilic compound appeared to be overcome by the addition of the excipient to the milling process. Another study confirmed that co-milling with a polymer can increase the wettability of a drug (Varghese and Ghoroi, 2017).

A limitation of this work is that it screened only one high- T_g glass former. More studies with high- T_g glass formers and different excipients are required to strengthen the hypothesis that dry co-milling is a suitable technique for the development of stable supersaturable formulations. The correlation between drug melting point depression with dissolution parameters also needs further investigation using other drug-excipient combinations. This correlation is only applicable for co-milled formulations which contain residual crystallinity, because fully amorphous systems do not have a melting point.

Future studies could investigate interactions between drug substances and excipients due to co-milling. Since the milled material remains in the solid state throughout the process, interactions at the molecular level might be less pronounced compared to formulations produced by spray drying or hot melt extrusion. Nonetheless, even weak interactions such as van der Waals forces or hydrogen bonds created by co-milling may have a significant impact on dissolution, especially when using a swellable excipient like croscarmellose sodium. These interactions could lead to favourable particle arrangements of co-milled material, particularly benefiting highly lipophilic and brittle drugs. Future research could investigate drug-excipient interactions generated by co-milling, as well as the influence of drug deformation behaviour on the degree of co-milling-induced lattice disorder.

Overall, this work demonstrated that co-milling of high- T_g glass formers such as apremilast appears to be a promising approach to produce stable formulations with supersaturation kinetics. The drug melting point depression correlated with the dissolution enhancement of this high- T_g glass former and may be a critical quality attribute for the design of partially crystalline formulations prepared by co-milling. Further, this study delivered additional data where a low- T_g drug lost to a much lower extent crystallinity due to the milling process compared to the high- T_g candidate, even though both compounds belong to glass forming ability class III. The addition of croscarmellose sodium to the milling process seemed not to have a positive effect on the stabilization of crystal lattice disorder of this lipophilic low- T_g compound but the dissolution was significantly improved.

5. Conclusion

This study showed that applying the same co-milling conditions on two stable glass formers with T_g s below and above milling temperature can lead to significantly different degrees of produced crystal lattice disorder. The low- T_g glass former fenofibrate remained mainly in an ordered crystalline state after one hour of co-milling and the dissolution rate enhancement correlated with the surface increase of the co-milled

system. A higher degree of structural disorder was measured for the high- T_g glass former apremilast and supersaturation kinetics during *in vitro* dissolution were observed. The milling induced entropy increase in crystal lattices led to a melting point depression, which highly correlated with the *in vitro* dissolution enhancement of co-milled apremilast. Thus, a co-milling related melting point depression may be a useful critical quality attribute for the production of co-milled formulations to assess the degree of process induced structural disorder and to anticipate drug supersaturation.

CRediT authorship contribution statement

Nicolas Pätzmann: Writing – original draft, Visualization, Validation, Software, Methodology, Investigation, Formal analysis, Data curation, Conceptualization. **Josef Beránek:** Writing – review & editing, Supervision, Resources, Project administration, Methodology, Investigation, Funding acquisition, Conceptualization. **Brendan T. Griffin:** Writing – review & editing, Visualization, Validation, Supervision, Project administration, Funding acquisition. **Martin Kuentz:** Writing – review & editing, Validation, Supervision, Resources, Project administration, Methodology, Investigation, Funding acquisition, Conceptualization. **Patrick J. O'Dwyer:** Writing – review & editing, Validation, Supervision, Project administration, Methodology, Investigation, Formal analysis, Conceptualization.

Declaration of competing interest

The authors report no declarations of interest.

Acknowledgements

This project has received funding from the European Union's Horizon 2020 research and innovation programme under the Marie Curie Skłodowska-Curie grant agreement No 955756.

We would like to thank Ondřej Dammer, Lukáš Krejčík and Hana Tožičková for their cooperation in XRPD, DSC and specific surface area measurements.

Supplementary materials

Supplementary material associated with this article can be found, in the online version, at [doi:10.1016/j.ejps.2025.107081](https://doi.org/10.1016/j.ejps.2025.107081).

Data availability

Data will be made available on request.

References

- Abushal, A.S., Aleanizy, F.S., Alqahtani, F.Y., Shakeel, F., Iqbal, M., Haq, N., Alsarra, I.A., 2022. Self-nanoemulsifying drug delivery system (SNEDDS) of apremilast: *in vitro* evaluation and pharmacokinetics studies. *Molecules*. 27, 3085. <https://doi.org/10.3390/molecules27103085>.
- Ahmed, E., Karothu, D.P., Pejov, L., Commins, P., Hu, Q., Naumov, P., 2020. From mechanical effects to mechanochemistry: softening and depression of the melting point of deformed plastic crystals. *J. Am. Chem. Soc.* 142, 11219–11231. <https://doi.org/10.1021/jacs.0c03990>.
- Alhalaweh, A., Alzghoul, A., Kaiyaly, W., Mahlin, D., Bergström, C.A.S., 2014. Computational predictions of glass-forming ability and crystallization tendency of drug molecules. *Mol. Pharm.* 11, 3123–3132. <https://doi.org/10.1021/mp500303a>.
- Alsayed, A.M., Islam, M.F., Zhang, J., Collings, P.J., Yodh, A.G., 2005. Premelting at defects within bulk colloidal crystals. *Science* (1979) 309, 1207–1210. <https://doi.org/10.1126/science.1112399>.
- Asgreen, C., Knopp, M.M., Skytte, J., Löbmann, K., 2020a. Influence of the polymer glass transition temperature and molecular weight on drug amorphization kinetics using ball milling. *Pharmaceutics*. 12, 483. <https://doi.org/10.3390/pharmaceutics12060483>.
- Asgreen, C., Knopp, M.M., Skytte, J., Löbmann, K., 2020b. Influence of the polymer glass transition temperature and molecular weight on drug amorphization kinetics using ball milling. *Pharmaceutics*. 12, 483. <https://doi.org/10.3390/pharmaceutics12060483>.
- Baird, J.A., Van Eerdenbrugh, B., Taylor, L.S., 2010. A classification system to assess the crystallization tendency of organic molecules from undercooled melts. *J. Pharm. Sci.* 99, 3787–3806. <https://doi.org/10.1002/jps.22197>.
- Balani, P.N., Ng, W.K., Tan, R.B.H., Chan, S.Y., 2010. Influence of excipients in comilling on mitigating milling-induced amorphization or structural disorder of crystalline pharmaceutical actives. *J. Pharm. Sci.* 99, 2462–2474. <https://doi.org/10.1002/jps.21998>.
- Bennett-Lenane, H., Koehl, N.J., O'Dwyer, P.J., Box, K.J., O'Shea, J.P., Griffin, B.T., 2021. Applying computational predictions of biorelevant solubility ratio upon self-emulsifying lipid-based formulations dispersion to predict dose number. *J. Pharm. Sci.* 110, 164–175. <https://doi.org/10.1016/j.xphs.2020.10.055>.
- Bhujbal, S.V., Mitra, B., Jain, U., Gong, Y., Agrawal, A., Karki, S., Taylor, L.S., Kumar, S., (Tony) Zhou, Q., 2021. Pharmaceutical amorphous solid dispersion: a review of manufacturing strategies. *Acta Pharm. Sin. B* 11, 2505–2536. <https://doi.org/10.1016/j.apsb.2021.05.014>.
- Blaabjerg, L.I., Lindenberg, E., Löbmann, K., Grohgan, H., Rades, T., 2016. Glass forming ability of amorphous drugs investigated by continuous cooling and isothermal transformation. *Mol. Pharm.* 13, 3318–3325. <https://doi.org/10.1021/acs.molpharmaceut.6b00650>.
- Blaabjerg, L.I., Lindenberg, E., Rades, T., Grohgan, H., Löbmann, K., 2017. Influence of preparation pathway on the glass forming ability. *Int. J. Pharm.* 521, 232–238. <https://doi.org/10.1016/j.ijpharm.2017.02.042>.
- Brokešová, J., Slámová, M., Zámotný, P., Kuentz, M., Koktan, J., Krejčík, L., Vraníková, B., Svačinová, P., Šklubalová, Z., 2022. Mechanistic study of dissolution enhancement by interactive mixtures of chitosan with meloxicam as model. *Euro. J. Pharmaceut. Sci.* 169, 106087. <https://doi.org/10.1016/j.ejps.2021.106087>.
- Chikhaliya, V., Forbes, R.T., Storey, R.A., Ticehurst, M., 2006. The effect of crystal morphology and mill type on milling induced crystal disorder. *Euro. J. Pharmaceut. Sci.* 27, 19–26. <https://doi.org/10.1016/j.ejps.2005.08.013>.
- Chipakwe, V., Semsari, P., Karlkvist, T., Rosenkranz, J., Chelgani, S.C., 2020. A critical review on the mechanisms of chemical additives used in grinding and their effects on the downstream processes. *J. Mater. Res. Technol.* 9, 8148–8162. <https://doi.org/10.1016/j.jmrt.2020.05.080>.
- Descamps, M., Willart, J.F., 2016. Perspectives on the amorphisation/milling relationship in pharmaceutical materials. *Adv. Drug Deliv. Rev.* 100, 51–66. <https://doi.org/10.1016/j.addr.2016.01.011>.
- Descamps, M., Willart, J.F., Dudogon, E., Caron, V., 2007. Transformation of pharmaceutical compounds upon milling and comilling: the role of tg. *J. Pharm. Sci.* 96, 1398–1407. <https://doi.org/10.1002/jps.20939>.
- Ejskjaer, L., O'Dwyer, P.J., Ryan, C.D., Holm, R., Kuentz, M., Box, K.J., Griffin, B.T., 2024. Developing an *in vitro* lipolysis model for real-time analysis of drug concentrations during digestion of lipid-based formulations. *Euro. J. Pharmaceut. Sci.* 194, 106681. <https://doi.org/10.1016/j.ejps.2023.106681>.
- Griffin, B.T., Kuentz, M., Vertzoni, M., Kostewicz, E.S., Fei, Y., Faisal, W., Stillhart, C., O'Driscoll, C.M., Reppas, C., Dressman, J.B., 2014. Comparison of *in vitro* tests at various levels of complexity for the prediction of *in vivo* performance of lipid-based formulations: case studies with fenofibrate. *Euro. J. Pharmaceut. Biopharmaceut.* 86, 427–437. <https://doi.org/10.1016/j.ejpb.2013.10.016>.
- Jagadish, B., Yelchuri, R.K.B., Tangi, H., Maroju, S., Rao, V.U., 2010. Enhanced dissolution and bioavailability of raloxifene hydrochloride by Co-grinding with different superdisintegrants. *Chem. Pharm. Bull. (Tokyo)* 58, 293–300. <https://doi.org/10.1248/cpb.58.293>.
- Kamil, M.M., Bayoumi, A.A., 2023. Co-milling: a successful approach to enhance solubility of a poorly soluble antihypertensive drug. *Indon. J. Pharm.* <https://doi.org/10.22146/ijp.7072>.
- Kasten, G., Lobo, L., Dengale, S., Grohgan, H., Rades, T., Löbmann, K., 2018. *In vitro* and *in vivo* comparison between crystalline and co-amorphous salts of naproxen-arginine. *Euro. J. Pharmaceut. Biopharmaceut.* 132, 192–199. <https://doi.org/10.1016/j.ejpb.2018.09.024>.
- Lentz, K.A., Plum, J., Steffansen, B., Arvidsson, P.O., Omkvist, D.H., Pedersen, A.J., Sennbro, C.J., Pedersen, G.P., Jacobsen, J., 2021. Predicting *in vivo* performance of fenofibrate amorphous solid dispersions using *in vitro* non-sink dissolution and dissolution permeation setup. *Int. J. Pharm.* 610, 121174. <https://doi.org/10.1016/j.ijpharm.2021.121174>.
- Lipson, S.G., Polturak, E., 2024. Experimental investigation of the premelting process in Sn. *Phys. Rev. B* 109, 024109. <https://doi.org/10.1103/PhysRevB.109.024109>.
- Löbmann, K., Laitinen, R., Strachan, C., Rades, T., Grohgan, H., 2013. Amino acids as co-amorphous stabilizers for poorly water-soluble drugs – Part 2: molecular interactions. *Euro. J. Pharmaceut. Biopharmaceut.* 85, 882–888. <https://doi.org/10.1016/j.ejpb.2013.03.026>.
- Murdande, S.B., Pikal, M.J., Shanker, R.M., Bogner, R.H., 2010. Solubility advantage of amorphous pharmaceuticals: I. A thermodynamic analysis. *J. Pharm. Sci.* 99, 1254–1264. <https://doi.org/10.1002/jps.21903>.
- Oliveira, P.F.M., Willart, J.F., Siepmann, J., Siepmann, F., Descamps, M., 2018. Using milling to explore physical states: the amorphous and polymorphic forms of dexamethasone. *Cryst. Growth Des.* 18, 1748–1757. <https://doi.org/10.1021/acs.cgd.7b01664>.
- Patterson, J.E., James, M.B., Forster, A.H., Lancaster, R.W., Butler, J.M., Rades, T., 2007. Preparation of glass solutions of three poorly water soluble drugs by spray drying, melt extrusion and ball milling. *Int. J. Pharm.* 336, 22–34. <https://doi.org/10.1016/j.ijpharm.2006.11.030>.
- Pätzmann, N., O'Dwyer, P.J., Beránek, J., Kuentz, M., Griffin, B.T., 2024. Predictive computational models for assessing the impact of co-milling on drug dissolution. *Euro. J. Pharmaceut. Sciences* 198, 106780. <https://doi.org/10.1016/j.ejps.2024.106780>.
- Priemel, P.A., Grohgan, H., Rades, T., 2016. Unintended and *in situ* amorphisation of pharmaceuticals. *Adv. Drug Deliv. Rev.* 100, 126–132. <https://doi.org/10.1016/j.addr.2015.12.014>.
- Slámová, M., Prausová, K., Epikaridisová, J., Brokešová, J., Kuentz, M., Patera, J., Zámotný, P., 2021. Effect of co-milling on dissolution rate of poorly soluble drugs. *Int. J. Pharm.* 597, 120312. <https://doi.org/10.1016/j.ijpharm.2021.120312>.
- Štukelj, J., Svanbäck, S., Agopov, M., Löbmann, K., Strachan, C.J., Rades, T., Yliuusi, J., 2019. Direct measurement of amorphous solubility. *Anal. Chem.* 91, 7411–7417. <https://doi.org/10.1021/acs.analchem.9b01378>.
- Suys, E.J.A., Chalmers, D.K., Pouton, C.W., Porter, C.J.H., 2018. Polymeric precipitation inhibitors promote fenofibrate supersaturation and enhance drug absorption from a type IV lipid-based formulation. *Mol. Pharm.* 15, 2355–2371. <https://doi.org/10.1021/acs.molpharmaceut.8b00206>.
- Tipduangta, P., Takiuddin, K., Fábán, L., Belton, P., Qi, S., 2015. A new low melting-point polymorph of fenofibrate prepared via Talc induced heterogeneous nucleation. *Cryst. Growth Des.* 15, 5011–5020. <https://doi.org/10.1021/acs.cgd.5b00956>.
- Varghese, S., Ghoroi, C., 2017. Improving the wetting and dissolution of ibuprofen using solventless co-milling. *Int. J. Pharm.* 533, 145–155. <https://doi.org/10.1016/j.ijpharm.2017.09.062>.
- Vogt, M., Vertzoni, M., Kunath, K., Reppas, C., Dressman, J.B., 2008a. Cogrounding enhances the oral bioavailability of EMD 57033, a poorly water soluble drug, in dogs. *Euro. J. Pharmaceut. Biopharmaceut.* 68, 338–345. <https://doi.org/10.1016/j.ejpb.2007.06.011>.
- Vogt, M., Vertzoni, M., Kunath, K., Reppas, C., Dressman, J.B., 2008b. Cogrounding enhances the oral bioavailability of EMD 57033, a poorly water soluble drug, in dogs. *Euro. J. Pharmaceut. Biopharmaceut.* 68, 338–345. <https://doi.org/10.1016/J.EJPB.2007.06.011>.
- Wytenbach, N., Kirchmeyer, W., Alsenz, J., Kuentz, M., 2016. Theoretical considerations of the Prigogine-Defay ratio with regard to the glass-forming ability of drugs from undercooled melts. *Mol. Pharm.* 13, 241–250. <https://doi.org/10.1021/acs.molpharmaceut.5b00688>.
- Yang, L., Wu, P., Xu, J., Xie, D., Wang, Z., Wang, Q., Chen, Y., Li, C.H., Zhang, J., Chen, H., Quan, G., 2021. Development of Apremilast solid dispersion using TPGS and PVPVA with enhanced solubility and bioavailability. *AAPS. PharmSciTech.* 22, 142. <https://doi.org/10.1208/s12249-021-02005-x>.
- Zhang, Q., Durig, T., Blass, B., Fassihi, R., 2022. Development of an amorphous based sustained release system for apremilast a selective phosphodiesterase 4 (PDE4) inhibitor. *Int. J. Pharm.* 615, 121516. <https://doi.org/10.1016/j.ijpharm.2022.121516>.
- Zhang, Q., Li, A., Yan, Y., Wu, Y., Zhang, X., 2021. Systematic thermodynamic analysis of apremilast polymorphs via solubility measurement with modeling: mechanism evaluation through molecular simulation. *Euro. J. Pharmaceut. Sci.* 165, 105958. <https://doi.org/10.1016/j.ejps.2021.105958>.
- Zimper, U., Aaltonen, J., Krauel-Goellner, K., Gordon, K.C., Strachan, C.J., Rades, T., 2010a. The influence of milling on the dissolution performance of Simvastatin. *Pharmaceutics*. 2, 419–431. <https://doi.org/10.3390/pharmaceutics2040419>.
- Zimper, U., Aaltonen, J., McGovern, C.M., Gordon, K.C., Krauel-Goellner, K., Rades, T., 2010b. Quantification of process induced disorder in milled samples using different analytical techniques. *Pharmaceutics*. 2, 30–49. <https://doi.org/10.3390/pharmaceutics2010030>.